THE ROLE OF DAMAGE MODE IN DELAYED DETONATION
OF COMPOSITE ENERGETIC MATERIALS

E. R. Matheson and J. T. Rosenberg
Lockheed Martin Space Systems Company
1111 Lockheed Martin Way
Sunnyvale, CA 94089

In addition to shock-to-detonation transition (SDT), solid propellants may detonate at significantly lower impact stresses than required for SDT. Detonation is delayed relative to SDT requiring a few shock transit times characteristic of the sample size. Since the delayed detonation mechanism is unknown, it is classified XDT for unknown-to-detonation transition. Although the exact mechanism is not known, it is clear that the shock stresses have diminished significantly by the time of the delayed detonation, and therefore, it is postulated that the material must be sensitized in some manner in order for it to detonate at the observed times. The primary candidate for sensitization is internal damage and its associated porosity generated by tensile waves[1]. Experiments designed to provide insight into the roles of various material damage mechanisms associated with delayed detonation are described here. In addition, the Tensile Damage & Distention (TDD) model[2,3] as implemented in the CTH shock physics code[4] has been modified and correlated to capture the essence of these experiments. The resultant correlated TDD model has been used to study a limited number of XDT experiments to assess the damage modes thought to be responsible for sensitizing the material.

INTRODUCTION

Some composite ductile solid rocket motor propellants exhibit delayed detonation or XDT when impacted onto steel plates. Relative to SDT events, these detonations occur at significantly lower impact velocities and with significantly longer delay times (typically a few shock transit times across the sample). XDTs are thought to occur because internal damage evolves and sensitizes the material, and subsequent loading and deformation of the damaged material initiate energy release leading to detonation buildup. To improve understanding of the damage processes in composite energetic materials, the Viscous-Elastic-Plastic (VEP) deformation model[5] was coupled to the Tensile Damage & Distention (TDD) model in the CTH shock physics code. The resultant VEP/TDD model was correlated to a select set of experiments and was then used to simulate a limited set of XDT experiments up to the time of detonation.

The first set of experiments conducted was for material characterization, and it included 1-D interrupted spall and 2-D Taylor rod impact experiments. The spall experiments provide data on failure at high stress and low strain, and the Taylor rod experiments provide data on failure at high strain and low stress. Both sets of experiments include failure modes thought to occur during XDT experiments.

XDT experiments were performed in which right circular propellant cylinders impact end-on against steel witness plates to find mean velocities for delayed detonation at four different scales. Measurements included time-resolved photography of sample deformation, radiographs at discrete times during sample deformation and detonation, time to detonation, witness plate stress histories, and witness plate crater topologies. None of these data yield direct measurements of the thermomechanical processes and states in the vicinity of the initiation site or elsewhere in the sample. Here, mechanisms for XDT are inferred from examination of the witness plate craters and simulation of damage evolution up to the time of detonation.

At the time of XDT, the propellant cylinder has experienced extensive mechanical deformation and damage. The witness plates provide evidence of the types of damage produced at the impact face. At the smallest scales tested, the craters are very smooth over most of the depression with scalloping exhibited around the periphery. These features are also typically observed at the largest scales tested. However, for similar impact velocities but much longer detonation times, the craters at the largest scale are extensively pockmarked over the entire surface. In general, there is an increasing density of pockmarks with increasing detonation time at this scale. The observed variability in time to detonation may be attributed to a small but measurable tilt angle at the impact face.

For small scales and shorter detonation times at large scale, most of the crater is very smooth implying the propellant experienced insufficient strain to fracture at the front face. Except for possible rear surface spall, the majority of the sample is thought to be unfractured, although extensive microdamage is predicted. The microdamage is postulated to be decohesion of energetic

crystals from the binder system. When a secondary shock wave passes through the damaged propellant, recompaction dissipates kinetic energy into heat through an undetermined process leading to a thermochemical response. A candidate process is grinding of crystals upon each other as they attempt to return to their original configurations.

For the longer detonation times at large scale, it is postulated that the propellant experienced greater deformation and consequently sufficient strains at the impact face to cause extensive fracturing. The pockmarks in the witness plates for these XDTs are thought to be the result of individual fragments detonating sympathetically. The initial energy release process could occur in either the fragmented or the intact (albeit with extensive microdamage) section of the sample. The same recompaction energy release mechanism might be responsible for the detonations occurring at longer times, but there could be another process. The partially fractured impact face produces conditions similar to those in a mechanical deflagration-to-detonation transition (DDT) experiment in which propellant fragments are loosely poured into a confining tube and impacted by a low-velocity piston. This is the XDT mechanism proffered in Reference 1.

The Tensile Damage & Distention (TDD) model in the CTH shock physics code provides a means for studying the two postulated damage processes in XDT experiments. TDD models damage using separate processes for particle-binder decohesion and binder scission. The first process cannot cause full damage as the binder is intact and can support very large strains. The total stresses used to drive the damage processes are provided by pressure computed in the CTH equation of state package[6] and the stress deviator tensor computed using the Viscous-Elastic-Plastic (VEP) model. TDD is first correlated to spall and Taylor rod impact experiments. Then, TDD is used to map out damage modes at the time of detonation in the smallest scale XDT experiments.

Here, it is postulated that kinetic energy is dissipated through crystal viscoplastic flow and fracture due to grinding action at the scale of the crystals. Recompaction of propellant fragments, however, probably dissipates energy through viscoplastic deformation of the binder at the scale of the propellant fragments. Consequently, there are two potentially unrelated physical mechanisms responsible for the observed XDT events.

TENSILE DAMAGE & DISTENTION MODEL

In order to match the experimental observations as closely as possible, it was found necessary to modify the TDD constitutive forms presented in Reference 2. Only the crack growth models were modified, so only those portions of TDD will be discussed here.

For TDD, we have defined the effective principle stress, strain rate, and strain. The effective principal stress and strain rate are the traces of the stress and strain rate tensors after the compressive components of the traces are set to zero. The effective strain is simply the integral of the effective strain rate.

In addition to strain induction, stress-induced decohesion damage is now allowed as well. A simple modification to the previous TDD constitutive model for decohesion crack growth gives:

$$\dot{R}_d = f_c c_o \left[1 - e^{-(\sigma_{eff} - \sigma_d^o)/\sigma_d^*} e^{-(\varepsilon_{eff} - \varepsilon_d^o)/\varepsilon_d^*} \right] \quad (1)$$

where, R_d is the decohesion crack radius, c_o is the bulk sound speed, f_c is a factor between zero and one, σ_{eff} is the effective principal stress, σ_d^o is the decohesion threshold stress, σ_d^* is the characteristic stress for decohesion, ε_{eff} is the effective principal strain, ε_d^o is the decohesion threshold strain, and ε_d^* is the characteristic strain for decohesion. The decohesion crack size is limited by a maximum amount of damage associated with decohesion.

For scission damage, the conceptual aspects of brittle fracture toughness[2,8] borrowed from the BFRACT damage model have been eliminated as a simplification. Instead, the scission crack growth rate model is conceptually identical to that for decohesion shown in Equation 1:

$$\dot{R}_s = f_c c_o \left[1 - e^{-(\sigma_{eff} - \sigma_s^o)/\sigma_s^*} e^{-(\varepsilon_{eff} - \varepsilon_s^o)/\varepsilon_s^*} \right] \quad (2)$$

where, R_s is the decohesion crack radius, σ_s^o is the decohesion threshold stress, σ_s^* is the characteristic stress for decohesion, ε_s^o is the decohesion threshold strain, and ε_s^* is the characteristic strain for decohesion. In the old TDD model form, decohesion and scission processes were assumed to occur simultaneously. This assumption has been replaced by the assumption that scission cannot occur until the maximum extent of decohesion possible has occurred.

All other aspects of TDD were left unchanged. The necessity for these changes and their effects on the simulation results will be discussed in the following sections.

SPALL EXPERIMENTS

A series of 1-D spall experiments were conducted on the study propellant using propellant disks that were 4.9 mm thick. The propellant targets were impacted by PMMA flyers that were 2.79 mm thick. At low velocity, the propellant disks are observed to form discrete cracks, but full spall across the span of the target diameter does not occur. As the flyer velocity is increased, the cracks

get larger and begin to coalesce. The flyer velocity was increased until the propellant target spalled into two separate pieces.

The TDD model was used to simulate the experiment in which the flyer velocity is at the threshold for full spall of the propellant target. Figure 1 shows the damage profile through the propellant after full spall has occurred. For the simulations performed here, decohesion damage was limited to 40% in TDD. In Figure 1, it can be seen that there is a region where damage exceeds the 40% limit for decohesion. In this region, scission has occurred and has gone to 100% damage at a singular point in the target. There is a plateau of maximum decohesion damage on either side of the scission region, and the damage decays to zero beyond the plateau. This behavior is a direct result of assuming that decohesion occurs to the maximum possible extent prior to scission as discussed previously. Since the strain field prior to damage and void formation is small, both types of damage in the spall test are caused by large tensile stresses.
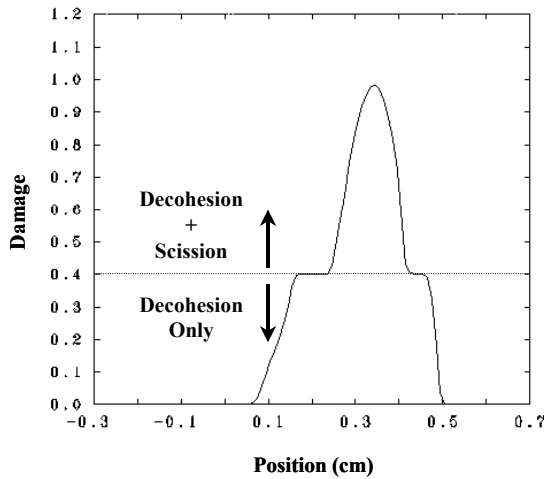

FIGURE 1. TDD DAMAGE PROFILE FOR 1-D SPALL TEST SIMULATION

TAYLOR ROD IMPACT EXPERIMENT

In Reference 7, the previous version of TDD was correlated to a Taylor rod experiment. In that correlation, TDD erroneously predicted a region of full damage in the back of the rod. TDD did correctly produce a circumferential crack at the mid-radius of the impact face that ran a short distance longitudinally, but the damage incorrectly spread across the outer half of the impact face.

At first, an attempt was made to use the rate-dependence of the scission damage process to eliminate the full damage region in the back of the rod. It was discovered that this region was experiencing a large hydrostatic tensile state due to superposition of release waves from the sides and the rear surface of the test specimen. Although initial damage and void formation diminished the stress field, the fracture stress criterion was decreasing even faster because of its dependence on the crack radius. Thus, the rate-dependent brittle fracture concept was eliminated from TDD.

Figure 2 shows a sequence of shadowgraphs from a Taylor rod experiment for an L/D=1.34. The rod is seen to deform quite significantly. This sequence does not show later images of the rod rebounding from the impactor clearly demonstrating the viscoelastic nature of the propellant. Figure 3 shows a cut-away view through the rod midplane. A circumferential crack due to scission of the binder is revealed as well as decohered large energetic crystals. This image also illustrates that the propellant recovered close to its original cylindrical shape again indicating a high degree of viscoelasticity.
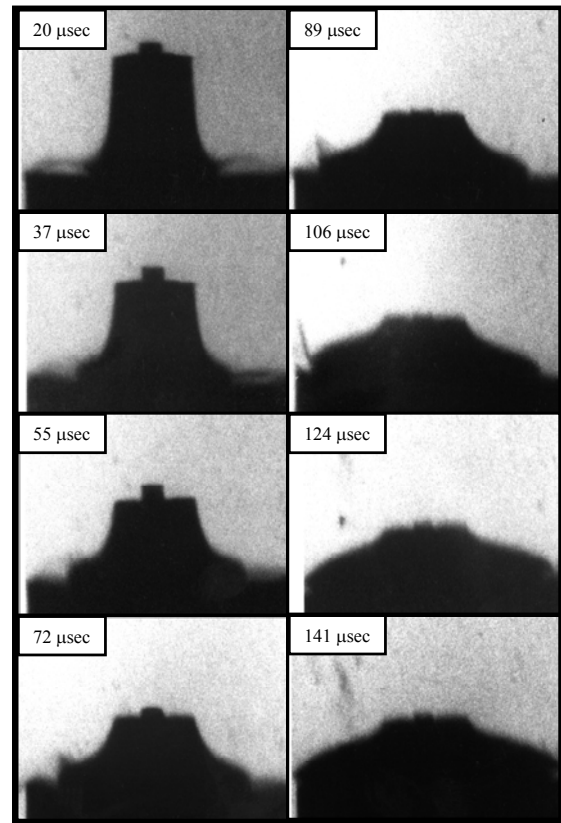
**FIGURE 2. TAYLOR TEST SHADOWGRAPH SEQUENCE**.
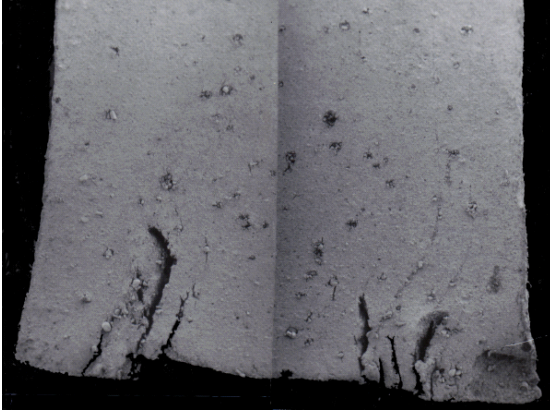
FIGURE 3. CROSS-SECTION OF TAYLOR ROD TEST SPECIMEN.

Figure 4 shows a simulated sequence for the Taylor rod experiment discussed above. The figure shows both deformed shapes and damage contours for comparison with Figures 2 and 3, respectively. At 20.0 µsec, the rod has largely suffered decohesion damage indicated by the gray area and has been engulfed by decohesion at 55.0 µsec. A circumferential crack due to full damage, i.e., scission, is evident at 125.0 µsec and later as a blackened region at the impact face. This scission damage is caused by strains exceeding 100% in TDD. The size and location of the crack agrees well with Figure 3. The rod foreshortening also agrees well with data (see Figure 2), but the spreading at the impact face is significantly underpredicted.

The TDD model was formulated with the notion of two distinct damage processes in order to match the Taylor test results. Without the decohesion process, the scission process as correlated to the spall test will always produce full damage on-axis at the impact face. Once the particles have decohered from the binder, porosity forms that greatly diminishes the local stress field, and the scission process is inhibited. This is a very important feature of the TDD model

It is not clear precisely why TDD underpredicts spreading. One plausible explanation is that the axial direction is in compression during this entire sequence while the radial and circumferential directions are in tension. Thus, the simple scalar distention model in TDD may be inadequate to predict this behavior accurately. However, to adopt a tensor description of distention would introduce immense complexities from both experimental and modeling perspectives.
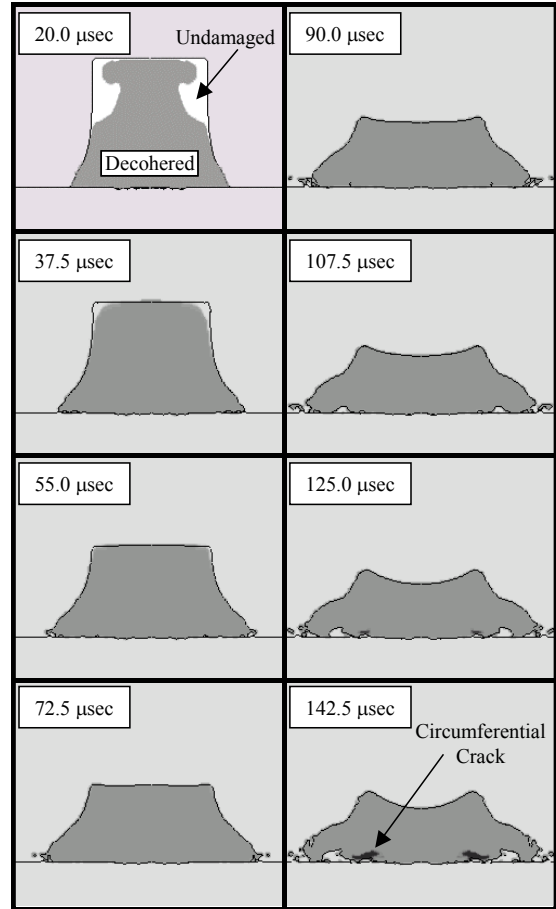

FIGURE 4. SIMULATION OF THE TAYLOR ROD IMPACT EXPERIMENT USING TDD.

25 mm SHOTGUN XDT EXPERIMENTS

Forward ballistics propellant impact experiments were performed at a 25 mm shotgun facility described in Reference 9. These experiments provided data on detonation responses and on deformation and damage as well.

Figure 5 shows a comparison of actual and simulated flash radiographs of the propellant deformed shape. For this experiment, the propellant cylinder impacted with a tilt angle of 10°, and yet, at the time of the flash radiograph, the deformed shape is reasonably symmetric in appearance. The simulation was performed in 2-D axisymmetric coordinates, and so, there is no tilt in the simulation. In spite of this, the comparison of deformed shapes is reasonable. As for the Taylor test, the change in length is very close, but the radial spreading is underpredicted. In this experiment, the propellant did not detonate probably due to the large tilt angle.
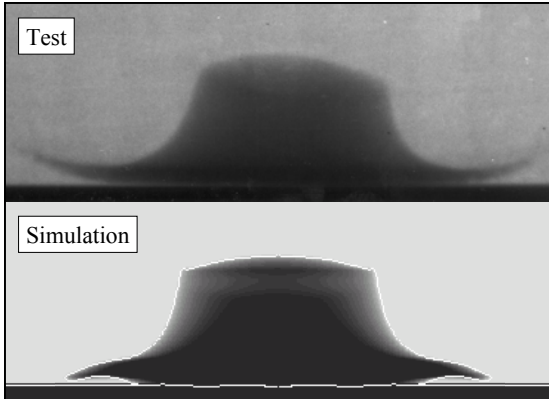
**FIGURE 5. MEASURED VS. SIMULATED DEFORMED SHAPE FOR 25 mm IMPACT.**

In order to gain further insight into the deformation and damage occurring at the impact face, a series of tests was conducted in which the propellant was fired at transparent targets. Figure 6 shows a sequence of photographs taken through a 38.1 mm thick Lexan target. Due to the lower shock stresses, there was no detonation, and the sample continued to spread radially outward for at least 260 μseconds. At the later times, it is apparent that there is significant damage in the form of circumferential cracks ringing the outer portions of the impact face. The interior portion does not appear to experience this type of damage. Although less prominent, it appears that this form of damage has already appeared at 60 μseconds or even sooner. This damage appears to be due to large radial strains and is consistent with the observations from the Taylor tests.
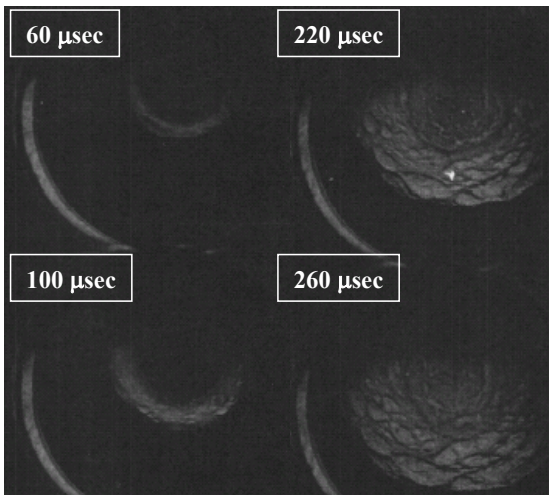
FIGURE 6. 25 mm PROPELLANT IMPACT FACE OBSERVED THROUGH LEXAN TARGET PLATE.

Further evidence of this damage mode may be found in the steel witness plates from 25 mm experiments in which XDT occurred. Figure 7 is a photograph of a crater for an experiment with a typical delay time for detonation. As for the clear target results,

there was apparently no cracking on the interior portion since that part of the crater is smooth. However, the outer portion of the crater exhibits a lot of scalloping. The scalloped nature of the outer edge is consistent with the fractures observed in the clear target data.
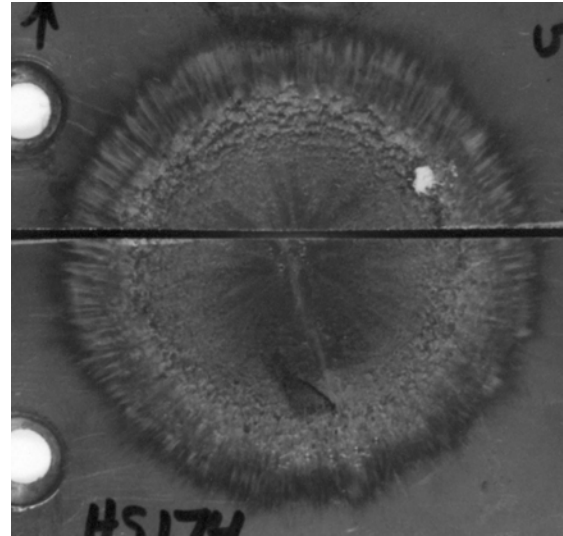

FIGURE 7. STEEL WITNESS PLATE CRATER FOR A 25 mm XDT EXPERIMENT.

Figures 8 and 9 show deformed shapes and damage contours at the time of detonation for the two experiments that had the longest and shortest detonation delay times, respectively. The shortest time is exactly half of the longest time. It also happens that these two experiments are near the extremes for lowest and highest velocities for XDT, respectively.
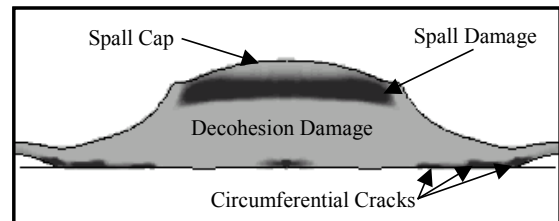
FIGURE 8. SIMULATED DEFORMATION AND DAMAGE FOR THE LONGEST DELAY 25 mm XDT EXPERIMENT.
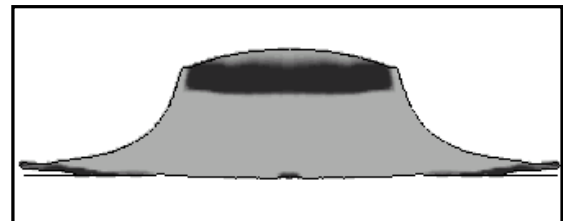
FIGURE 9. SIMULATED DEFORMATION AND

DAMAGE FOR THE SHORTEST DELAY 25 mm XDT EXPERIMENT.

Both cases show spall cap formation at the back of the sample that occurs early when the shock wave reflects off the rear surface. The pronounced bulge at the back surface is due to the spalled material separating in the middle but remaining attached at the radial edge. This bulge is apparent in the flash radiograph in Figure 5 but is not seen in the Taylor rod experiments in which spall damage did not occur. In Figure 8, several circumferential cracks have formed at the impact face periphery due to full scission damage caused by local strains exceeding 100%. In Figure 9, a single circumferential crack is observed at the impact face. In both cases, a small region on-axis at the impact face has achieved full damage. This damage is not observed directly and may be due to numerical problems in the simulations. The remainder of the sample throughout in both cases has experienced decohesion damage. These simulations are showing that the scalloped features at the periphery of the witness plate craters are due to circumferential cracks caused by strain damage. The smooth portion of the crater is created by material that has only experienced decohesion damage.

Previous work[7,9] has shown that the delayed detonation most probably initiates somewhere along or near the axis (depending on tilt angle) but not in the spall cap region. Combined with the results here, the implication is that delayed detonation initiates in a region where only decohesion damage has occurred.
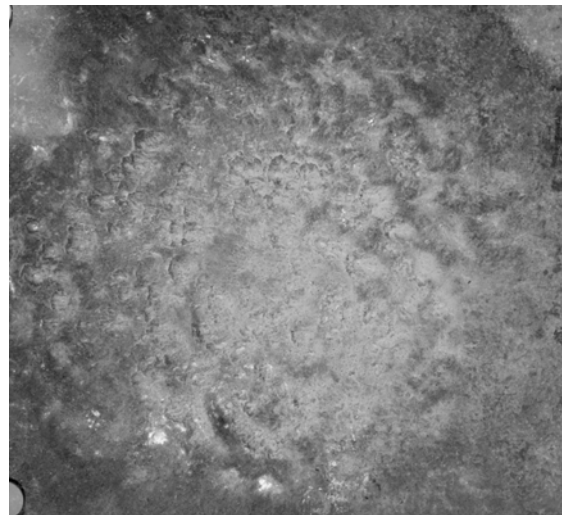
300 mm XDT EXPERIMENTS

XDT experiments were also conducted at the scales of 70 mm, 140 mm, and 300 mm. The first two sizes were tested in forward ballistics mode similarly to the 25 mm experiments using powder gun facilities. Because of sheer size, the 300 mm experiments were conducted using a rocket sled facility in reverse ballistics mode. The 300 mm samples were slung over the track, and the rocket sled propelled a stack-up of steel plates into the propellant sample. This configuration allowed more precise control of the impact tilt angles, and consequently, test results were more repeatable than at the other scales.

Figure 10 shows a photograph of a witness plate crater for a 300 mm XDT. This crater is virtually indistinguishable in character from that shown for a 25 mm XDT in Figure 7. Figure 11 shows another crater type from a 300 mm experiment that was not observed at the 25 mm scale. It exhibits a relatively uniform density of pockmarks over the entire crater surface. The impact velocity for this experiment was approximately 10% higher than that for the experiment that produced the crater in Figure 10, and yet, the time to detonation was more than twice as great as for the other experiment. This result is irrational unless one considers the tilt angle which was ~1.6° for this experiments versus ~1.0° for the

other experiment. It is thought that the tilt angle significantly delayed the time to detonation giving the propellant more time to spread over the witness plate. The strains became sufficient to cause the impact face to suffer massive scission damage, i.e., it turned to rubble. The pockmarks are evidence of individual fragments detonating. It is not known if the detonation is initiated in the rubble or at a location that only experienced decohesion damage. This crater type forces one to consider that there might be two modes of delayed detonation initiation, one associated with each of the damage modes.
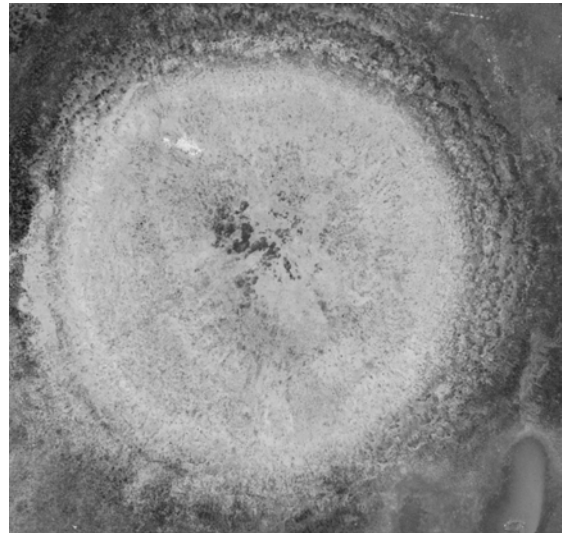
FIGURE 10. NORMAL STEEL WITNESS PLATE CRATER FOR A 300 mm XDT EXPERIMENT.

FIGURE 11. POCKMARKED STEEL WITNESS PLATE CRATER FOR A 300 mm XDT EXPERIMENT.

DISCUSSION

The TDD model has been calibrated to 1-D spall experiments and appears to give a reasonable simulation of the rear surface behavior in the XDT experiments. It is not thought that detonation initiates in the vicinity of the predicted spall caps, but the mechanical response in this region has a strong effect on the overall deformation of the propellant sample. In turn, the deformation response drives the damage response at the impact face and elsewhere. Thus, it is important to model the spall behavior with reasonable accuracy.

At first appearance, the dominant feature of the post-test sectioned Taylor rod is the circumferential crack at the impact face. Less apparent is decohesion around the energetic crystals. Careful examination reveals large crystals that are unseated from the binder. It is certainly possible than the particles separated during post-test sectioning. However, dynamic tensile tests in which the sample volumes were monitored revealed that at about 2% strain the samples begin to experience significant volume growth implying that internal porosity is forming. This observation led to the two-process damage approach used by TDD. Without the decohesion process, TDD would predict full damage on-axis in the Taylor rod impact test which is not observed. Like spall cap formation, the most important aspect of the large circumferential crack is its affect on overall deformation and formation of new release surfaces.

The XDT simulations performed with TDD produced two primary features observed in the experiments: 1) a prominent bulge at the rear surface, and 2) circumferential cracks at the periphery of the impact face as evidenced by the witness plate crater. The first feature is due to spall, and the second feature is due to strain damage. TDD was first calibrated to the spall and Taylor rod experiments and, then, was used without adjusting any parameters to produce the XDT simulations. These TDD simulations provide credible evidence that the predominant damage mode on the interior of the test specimen is decohesion damage. Thus, it appears that most XDTs are probably caused by shearing and fracturing of energetic crystals as they attempt to reseat in their original configurations. An exception might be the XDTs at the 300 mm scale that produced a large number of pockmarks in the witness plate craters. These XDTs could possibly be caused by recompaction of the resultant large fragments.

In Reference 1, it was suggested that damage and porosity evolution could be responsible for sensitizing the propellant during XDT impact experiments. After the material is sensitized, low level shocks could easily cause a detonation. It was postulated that the mechanism might be recompaction similar to buildup to detonation in piston-driven DDT experiments. As a result, DDT experiments were included in the test program. The porous beds for these tests were comprised of manufactured fragments that were loosely poured into a Lexan tube. The resultant bed densities were approximately 60% TMD. These experiments produced detonations, but in retrospect, the initial states of the porous beds appear more similar to the conditions at the impact face for the XDTs that produced lots of pockmarks in the witness plate. Unfortunately, no reactive experiments have been conducted that replicate the sensitization inherent to the pure decohesion damage mode. In order to construct predictive tools for XDT simulation, experiments that characterize buildup to detonation in prestrained, decohered propellant should be conducted.

There appears to be a strong dependence on tilt angle at all scales tested. The 25 mm experiment shown in Figure 5 was conducted at a velocity that was right in the middle of the XDT range, and yet, there was no detonation. This experiment had a large tilt angle of 10°. At the 300 mm scale, the experiment that produced a lot of pockmarks was for a higher velocity than the other experiment, but it had a much longer delay time to detonation. This experiment had one of the larger tilt angles measured for the 300 mm experiments. The next step for this effort is to correlate the Coupled Damage and Reaction (CDAR) model[7,10] to these experiments. In order to correlate to individual experiments, it appears that it will be necessary to eventually perform 3-D CDAR calculations accounting for the tilt angle. This will be a computationally demanding exercise. It might also prove necessary to modify CDAR to include two recompaction initiation terms in its burn model, one for each type of damage discussed here.

SUMMARY AND CONCLUSIONS

The TDD model has been calibrated to spall and Taylor rod impact experiments for a solid rocket propellant representing two distinct damage modes. The TDD model was then used to simulate 25 mm XDT experiments, and it successfully replicated damage responses inferred from deformed shapes and features in witness plate craters. These simulations predict that the delayed detonations probably initiate in a region that has experienced only decohesion damage, i.e., a region where the binder remains intact. For some XDT experiments at large scale, there may be another initiation mode caused by recompaction of propellant fragments, i.e., fully damaged propellant.

The decohesion mode was not anticipated during planning for the test program, and consequently, there are no data for construction of reaction buildup models for this mechanism. If possible, this deficiency eventually needs to be addressed. If not, then the XDT experiments will be used to correlate rather than validate the CDAR coupled damage and reaction model.

The success of the TDD model in replicating the observed XDT damage modes is very encouraging. Since, TDD forms the damage portion of the CDAR model, it was important to calibrate and validate TDD against experimental data before starting the reactive simulations. Calibration of the reactive portion of CDAR will be the next phase of our program.

ACKNOWLEDGMENTS

REFERENCES

1. Green, L. G., James, E., Lee, E. L., Chambers, E. S., Tarver, C. M., Westmoreland, C., Weston, A. M., Brown, B., "Delayed Detonation in Propellants from Low Velocity Impact," Seventh Symposium (International) on Detonation, Annapolis, MD, 16-19 June 1981, pp.256-264.
2. Matheson, E. R., Drumheller, D. S., and Baer, M. R., "An Internal Damage Model for Viscoelastic-Viscoplastic Energetic Materials," in *Shock Compression of Condensed Matter - 1999*, edited by M. D. Furnish, L. C. Chhabildas, and R. S. Hixson, AIP Conference Proceedings 505, New York, 1999, pp. 691-694.
3. Matheson, E. R., Drumheller, D. S., and Baer, M. R., "A Viscoelastic-Viscoplastic Distention Model for Granulated Energetic Materials," *Proceedings of the JANNAF 18th Propulsion Systems Hazards Subcommittee (PSHS) Meeting*, Cocoa Beach, FL, 18-21 October, 1999.
4. Hertel, E. S., et al., "CTH: A Software Family for Multi-Dimensional Shock Physics Analysis," in *Proceedings of the 19th International Symposium on Shock Waves*, edited by R. Brun and L. D. Dumitrescu, pp.377-382.
5. Olsen, E. M., Rosenberg, J. T., Kawamoto, J. D., Lin, C. F., Seaman, L., "XDT Investigation by Computational Simulation of Mechanical Response Using a New Viscous Internal Damage Model," Eleventh Symposium (International) on Detonation, Snowmass, CO, 31 August-4 September, 1998, pp. 170-178.
6. Kerley, G. I., "CTH Reference Manual: The Equation of State Package," SAND91-0344, May 1991.
7. Matheson, E. R., and Rosenberg, J. T., "A Mechanistic Study of Delayed Detonation in Impact Damaged Solid Rocket Propellant," in *Shock Compression of Condensed Matter - 2001*, AIP Conference Proceedings, pending release.
8. Seaman, L., Simons, J. W., Erlich, D. C., Olsen, E. M., Rosenberg, J. T., Matheson, E. R., "Development of a Viscous Internal Damage Model for Energetic Materials Based on the BFRACT Microfracture Model," Eleventh Symposium (International) on Detonation, Snowmass, CO, 31 August-4 September, 1998, pp. 632-639.
9. Matheson, E. R., Rosenberg, J. T., Ngo, T. A., and Butcher, G., "Programmed XDT: A New Technique to Investigate Impact-Induced Delayed Detonation," *Eleventh Symposium (International) on Detonation*, Snowmass, CO, 30 August – 4 September, 1998, pp. 162-169.
10. Matheson, E. R., Drumheller, D. S., and Baer, M. R., "A Coupled Damage and Reaction Model for Simulating Energetic Material Response to Impact Hazards," in *Shock Compression of Condensed Matter - 1999*, edited by M. D. Furnish, L. C. Chhabildas, and R. S. Hixson, AIP Conference Proceedings 505, New York, 1999, pp. 651-654.